UC Riverside
UC Riverside Previously Published Works

Title

Cell Division Resets Polarity and Motility for the Bacterium Myxococcus xanthus

Authors

Harvey, Cameron W
Madukoma, Chinedu S
Mahserejian, Shant
et al.

Cell Division Resets Polarity and Motility for the Bacterium *Myxococcus xanthus*

Cameron W. Harvey,[a,b] Chinedu S. Madukoma,[c] Shant Mahserejian,[a] Mark S. Alber,[a,b,d] Joshua D. Shrout[c,e]

Department of Applied and Computational Mathematics and Statistics, University of Notre Dame, Notre Dame, Indiana, USA[a]; Department of Physics, University of Notre Dame, Notre Dame, Indiana, USA[b]; Department of Civil and Environmental Engineering and Earth Sciences, University of Notre Dame, Notre Dame, Indiana, USA[c]; Department of Medicine, Indiana University School of Medicine, Indianapolis, Indiana, USA[d]; Department of Biological Sciences, University of Notre Dame, Notre Dame, Indiana, USA[e]

Links between cell division and other cellular processes are poorly understood. It is difficult to simultaneously examine division and function in most cell types. Most of the research probing aspects of cell division has experimented with stationary or immobilized cells or distinctly asymmetrical cells. Here we took an alternative approach by examining cell division events within motile groups of cells growing on solid medium by time-lapse microscopy. A total of 558 cell divisions were identified among approximately 12,000 cells. We found an interconnection of division, motility, and polarity in the bacterium *Myxococcus xanthus*. For every division event, motile cells stop moving to divide. Progeny cells of binary fission subsequently move in opposing directions. This behavior involves *M. xanthus* Frz proteins that regulate *M. xanthus* motility reversals but is independent of type IV pilus "S motility." The inheritance of opposing polarity is correlated with the distribution of the G protein RomR within these dividing cells. The constriction at the point of division limits the intracellular distribution of RomR. Thus, the asymmetric distribution of RomR at the parent cell poles becomes mirrored at new poles initiated at the site of division.

Many approaches to study cell division utilize traits that readily allow the distinction of two progeny cells. For example, cells displaying "asymmetrical" division traits allow the clear distinction of numerous characteristics that can then be monitored while deciphering other unknowns. *Caulobacter* bacteria are among the best studied with this distinction (1), but other biological examples include: preneuron neuroblast brain cells, budding *Saccharomyces cerevisiae*, germ line cells of male *Drosophila*, endospore development by *Bacillus* species, and *Mycobacterium* species subjected to environmental nutrient stress (2, 3). While such explicitly distinct examples may be rare, nearly all types of cells display some asymmetrical properties when functioning properly. There are numerous examples of distinctive asymmetrical and polarized attributes of cells (4). However, one difficulty that remains in characterizing asymmetrical properties in biology is distinguishing the timing and order of those intra- and intercellular attributes that are transient in nature. Alternative to studying asymmetric cell types that can be readily differentiated, other research strategies to probe stages of division often examine stationary or immobilized cells.

Myxococcus xanthus is one of many myxobacteria, common soil microbes that grow readily in environments rich in complex organics, such as those containing decaying plants (5) or other bacteria (6). *M. xanthus* cells exhibit a symmetric morphology. The specific mechanism and dynamics of *M. xanthus* cell division, like those of most nonmodel organisms, are not entirely known. *M. xanthus* is among many bacteria lacking a clear MinCD system that drives the recruitment of FtsZ for division. It is known that the middle of *M. xanthus* cells is marked by PomZ, which likely recruits FtsZ (7) for proper division.

M. xanthus has been studied largely as a model organism to understand cellular motility and the development of self-organized swarming groups that aggregate to form sporulating fruiting bodies. Upon starvation, *M. xanthus* glides in a well-choreographed manner to aggregate into clusters containing roughly 10^6 cells, which then develop into *M. xanthus* fruiting bodies (8–13). *M. xanthus* does not move by flagella but displays two distinct motility phenotypes described as A motility and S motility. During A motility, cells move with or without the company of neighbor cells and do so preferentially in tracks of polysaccharide slime; the specific mechanism(s) of A motility remains under investigation, and proposed models include propulsion by slime secretion, focal adhesions, or a helical motor (14–17). During S motility, *M. xanthus* cells attach to other cells by using type IV pili (TFP) at the leading pole to pull the cell forward when the pilus tips have bound to exopolysaccharide covering cells ahead (18–20). Another important facet of *M. xanthus* movement is that this bacterium regularly reverses direction (21); during reversal, the leading and lagging poles switch in seconds (21–23). Reversals have been traced to the action of a small G-protein switch (24, 25), and these reversals are induced by the Frz system (26–28). At the core of the Frz system is a two-component signal transduction system consisting of FrzCD, a methyl-accepting chemoreceptor domain, and FrzE, a histidine-kinase protein (29–31). The Frz proteins are homologous to Che proteins that confer swimming chemotaxis on several bacteria (32, 33). However, the Frz signal-transducing proteins lack an extracellular receptor to confer classical chemotaxis (26, 29), which is similar to other signal transduction networks, such as Wsp in *Pseudomonas aeruginosa*, where the input mechanism has not been fully elucidated (34–36). Several proteins asso-

TABLE 1 Strains used in this study

M. xanthus strain	Relevant characteristic(s)	Source or reference
DK1622	A$^+$ S$^+$; wild-type strain	62
DZ2	A$^+$ S$^+$; wild-type strain	8
DK8621	A$^+$ S$^-$; Δ*pilA* mutant of DK1622	Kaiser collection, Wall laboratory
DK7881	Hyporeversing Δ*frzE* mutant of DK1622	63
DW706	Hyperreversing Δ*frzCD* mutant of DK1622 (Mx4 transduction of *frzCD*::Tn*5*-132 Ω224)	Wall laboratory
DK1240	A$^-$ S$^+$; Δ*cglC6* mutant of DK1622	56
DZ4483	Hyporeversing Δ*frzF* mutant of DZ2	29
DZ4482	Hyperreversing Δ*frzG* mutant of DZ2	29
JS1	P$_{nat}$-*romR*-GFP fusion in DK1622 (constructed with pSH1208)	This study[a]
JS2	P$_{nat}$-*romR*-GFP fusion in DW706 (constructed with pSH1208)	This study[a]

[a] Obtained by using the approach described in reference 24.

ciated with motility and reversals of *M. xanthus* have been shown to display localized traits (24, 25, 27, 28, 37–40); however, the biochemistry and regulation governing motility behavior of *M. xanthus* continues to be investigated. The ability to reverse has been shown to be crucial in maximizing the overall spreading of *M. xanthus* populations by minimizing and resolving collisions.

Here we investigated *M. xanthus* cell division under conditions that promote surface motility. We report that cell division and surface motility are coordinated for the bacterium *M. xanthus* as polarity is reset at the time of division. We demonstrate that when they are surface motile, *M. xanthus* cells always pause their movement to complete binary cell division. Further, these dividing *M. xanthus* cells display asymmetrical properties with respect to inherited polarity. After a consistent period, the two progeny cells are predisposed to resume movement in opposing directions. These pauses for division dominate over any intercellular interactions, as even cells that are part of a motile cluster of cells will dissociate and stop prior to cell division. These pausing and polarity behaviors involve the Frz reversal proteins FrzCD and FrzE but are independent of TFP-mediated *M. xanthus* S motility. While the timing basis for these division pauses is currently unclear, these dividing cells plainly display asymmetric properties that coincide with cell division. We demonstrate that opposing polarity of new progeny cells involves an asymmetric distribution of the G protein RomR as parent cell polar distributions of RomR become mirrored in new poles initiated at the site of division.

MATERIALS AND METHODS

Bacterial strains and growth medium. All of the strains of *M. xanthus* utilized for this study are included in Table 1. Strains were maintained by growth on CTT agar plates (41).

Imaging chamber assembly and inoculation. The imaging chambers used were adapted from the imaging plate complex described by Taylor and Welch (42). Briefly, we constructed a modified imaging chamber by using 20-mm-diameter and 2.0-mm-thick Grace Bio-Labs (Bend, OR) silicone gaskets. Sterile, melted CTT agar (2%) was pipetted into the gasket fixed to a microscope slide. A second microscope slide was place on top of the gasket, sandwiching the agar and the gasket between two slides. The assembly was held together by black metal binder clips and stored at 4°C to cure.

For inoculation, a chamber was moved from 4°C storage and warmed

to room temperature before removal of the top coverslip. Chambers were inoculated with *M. xanthus* by using a sterile platinum wire. The uncovered chamber was placed in an empty petri dish and sealed with Parafilm to limit agar drying. Immediately prior to imaging, a coverslip was placed on the chamber and pressed firmly around the perimeter to seal the thin agar disc (a thin liquid layer formed between the coverslip and the agar disc).

Cell division measurements. Tracking of cell division was done manually by screening individual frames of time-lapse movies of *M. xanthus*, which typically included 50 to 100 cells near the swarm edge in the imaging chambers used. The position, direction, and initial stoppage time of each parent cell were noted. Dividing cells in which the complete division sequence could not be chronicled were excluded from further analysis.

The two progeny cells were then designated with respect to the last known movement direction of the parent cell. The leading half of the cell was designated the "leading" cell, while the trailing half was designated the "lagging" cell. The cell was observed until both progeny cells initiated movement, and the time and direction (with respect to the parent) of each new cell were recorded. Despite this straightforward approach, interaction of dividing cells with neighboring cells presented the additional challenge of distinguishing between active movement by any cell from passive movement brought about by the movement of surrounding cells. To measure the pause duration of a division, we measured the number of frames between that last observed motion of the parent cell and the resumption of motion by either of the two progeny cells (the recorded pause duration does not include the extra time needed for the second progeny cell to resume motion).

Polarity inheritance measurements. The polarity of newly divided cells was compared to the last direction recorded for the predivision parent cell. The polarity of the parent cell was assigned according to the last observed moving direction. Accordingly, the polarity of the new cells was assigned on the basis of their initial movement direction in reference to the parent cell.

We recorded the motility start time of each newly divided cell independently. While many division events showed initiation of movement by both progeny cells in the same frame of the time-lapse data, more than half of the data showed one progeny cell initiating movement before the other. To distinguish between synchronous and asynchronous motility, events were identified as (i) leading cell starting first, (ii) lagging cell starting first, or (iii) both progeny cells starting together (synchronous). In order to establish a clear priority among the restarts, a threshold of 30 s between motility events was chosen before cells were counted as asynchronous.

Dynamic analysis of RomR distribution. RomR-green fluorescent protein (GFP) was tracked over the length of strain JS1 cell division. Each predivision sequence was manually delineated from the rest of the image in all frames. This segmented sequence was then processed by using a custom Matlab program to assign the delineated cell in each frame to a line representing the central longitudinal axis of the cell. Separately in ImageJ, the green fluorescent channel was processed by using the "despeckle" function, followed by filtering with a Gaussian blur to smooth the image. The linear distribution of RomR was obtained by averaging the fluorescence intensity of RomR-GFP over numerous blocks of three by three pixels centered on each pixel of the central axis line of a cell. This cell central axis line was then sectioned into 60 equally spaced points where 0 corresponded to the head (leading pole) of the cell and 1 corresponded to the tail (lagging pole). After a clear separation of progeny cells, the original 60 points were split into 30 points for each progeny cell, where 0 to 0.5 corresponded to the leading pole and 0.5 to 1 corresponded to the lagging pole. RomR-GFP intensity was spatially quantified as the fluorescent intensity at each of the 60 points along the 0-to-1.0 relative cell length. The dynamic intensity was obtained for all of the frames of a time-lapse movie and plotted by using the surface plot in Matlab.

RomR distribution was also analyzed to consider the relative abundance of RomR over a sequence of a dividing cell and its two progeny cells. We considered the two (old) poles of the parent cell and the cell midpoint

from which two new poles will form, the dividing cell midpoint, and the subsequent two new poles. Localized RomR levels were measured within areas of 10 by 10 pixels centered on each of these three localization foci. The mean GFP intensity was measured in the box in each frame of the image sequence. For these larger-area measurements, background subtraction was applied to each measurement by selecting a region of 10 by 10 pixels away from the cell. Relative abundance was normalized by dividing each measurement (three compartments, 48 frames) by the mean RomR-GFP intensity measured in frame 1 of the lagging-pole compartment of the predivision images. For the postdivision sequence, we normalize by dividing each measurement (two compartments, 30 frames) by the mean RomR-GFP intensity in frame 6 of the lagging cell's new pole compartment (i.e., the first frame where the two poles are distinguishable).

The ratio of the intensities of the leading and lagging poles was averaged over multiple frames prior to the point of separation. Contact with neighboring cells (and thus RomR signal coming from other cells) interfered with measurements during the division pause, limiting the number of frames available for certain division sequences. Following division, the first four frames in which the two new poles could be distinguished were used to get the average ratio of the leading cell's new pole to the lagging cell's new pole.

Growth rate. The surface growth rate of each strain was obtained by quantifying fluorescence over time by a fluorescence-imaging method (43). Briefly, *M. xanthus* colonies were grown on one 150-mm CTT agar (1.5%) plate containing 8 μl/100 ml of Syto64 bacterial-staining dye (Life Technologies, Grand Island, NY). Fluorescent images of swarm plates were acquired with a Carestream Multispectral FX imaging station (Carestream Health, Woodbridge, CT) by using excitation and emission wavelengths of 590 and 670 nm, respectively. Time-lapse images of the whole plate were recorded every 10 min. The growth rate of each strain was determined by calculating the mean fluorescent intensity of three replicates of each strain.

Velocity measurements. Fifteen to 20 cells of each strain were tracked manually by using the ImageJ plugin MtrackJ from a representative time-lapse data set. The leading edge of a tracked cell was identified in approximately 40 successive frames to calculate the average velocity of each tracked cell. The average velocity of the strain was then determined by averaging the velocities of all of the tracked cells. Because of the hyperreversing attributes of Δ*frzCD* mutant strain DW706, only 10 to 15 frames could typically be tracked before the cell reversed direction—for this strain, fewer frames (i.e., 10 to 15) were tracked, so more cells (i.e., 30) were used to calculate the average cell velocity. These measured velocities were representative of the cell speeds of these strains when they were grown and imaged in our chambers described above. Certainly, some differences in cell speed can be expected from previous reports in the literature, given the different environmental conditions of our chamber experiments. However, all of the cell speed data presented here provide the relative speeds of strains examined in this work, which was conducted under the same conditions as the division measurements.

Expansion measurements. The expansion or swarming rate of each strain was obtained by a protocol similar to that used in reference 44. A fresh agar plate was stab inoculated with a platinum wire containing growing *M. xanthus* cells. Over the course of 1 to 2 weeks, the diameters of the expanding colonies were measured with a ruler.

Statistical analysis. The pause durations of the *M. xanthus* strains studied were analyzed with analysis of variance (anova1) to determine that the different data sets do not have the same distribution. To determine which strains were significantly different from each other, a mean comparison (multcompare function in Matlab, which used results from anova1) was used to determine whether or not the 95% confidence intervals of the means of any two strains overlapped. Nonoverlapping intervals were recognized as significantly differing.
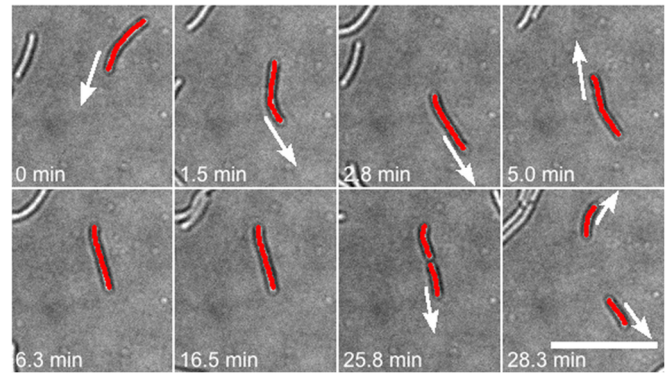

FIG 1 Sequence of motility pausing and cell division in one representative *M. xanthus* DK8621 cell. From the start of tracking (0 min), the cell moves in several directions, stops movement at 6.3 min, and divides at roughly 25 min and cells are clearly motile at 28.3 min. Scale bar, 10 μm.

RESULTS

***M. xanthus* cells pause to divide.** While imaging *M. xanthus* growing under nutrient-rich, motility-favoring conditions by using time-lapse microscopy, we observed that motile cells stop as a precursor step to binary cell division. Figure 1 shows a representative example where a motile *M. xanthus* cell pauses and remains paused until it has completed binary division (for a movie of the entire time-lapse series, see Movie S1 in the supplemental material). We subsequently probed for *M. xanthus* cell division events by systematically analyzing the movement of approximately 12,000 cells. While similar stoppage of predivision cells has been observed previously by Reichenbach et al. (45), our analysis shows that this is not an occasional or random event. Every dividing cell ($n = 558$) in our experiments paused prior to this division—no cells were observed to divide while motile. On average, for two common *M. xanthus* wild-type strains, DK1622 and DZ2, these motility pauses were approximately 19 min in duration before the two daughter cells resumed movement (Table 2). Further, only predivision cells paused for these extended durations. Motile, nondividing cells that stopped (either to reverse direction or continue in the same direction) all exhibited a pause duration of less than 1 min, which is in the range of reversal pauses that have been specifically measured previously (46, 47).

The requirement and duration of these pauses are notably unaffected by physical interactions with other *M. xanthus* cells. Predivision cells that are moving over surfaces in clusters dissociate from clusters and stop. Yet this stoppage is not a rigid, immovable fixation of cells to the surface, as stopped cells can be "jostled" or partially displaced. In general, however, predivision cells are notably unaffected by physical interactions with other *M. xanthus* cells. Dividing cells located within either low- or moderate-density populations show the same behavior as isolated cells. Key stages showing active motility, pausing of motility, interaction of paused cells with other motile cells, cell division, and resumption of motility after division for four different parent cells in the same field of view are included in Fig. 2 (for the entire sequence, see Movie S2 in the supplemental material). We found that group interactions are secondary to unicellular behavior associated with *M. xanthus* cell division—pausing for cell division was dominant over any intercellular interaction. Additionally, no distinction in the pausing behavior was found between dividing cells that were

TABLE 2 Predivison pauses, motility, and growth attributes of *M. xanthus* strains[a]

Strain	Pause duration (min)	Single-cell velocity (μm/min)	Group expansion rate[b] (μm/min)	Growth doubling time[b] (h)
DK1622	18.3 ± 0.8 (101)	5.04 ± 0.37 (19)	1.34 ± 0.25	4.8 ± 0.6
DZ2	19.7 ± 0.8 (90)	4.61 ± 0.62 (15)	1.60 ± 0.49	3.6 ± 0.1
Δ*pilA* mutant DK8621	17.2 ± 0.8 (97)	2.95 ± 0.67 (15)	0.90 ± 0.24	4.4 ± 0.4
Δ*frzE* mutant DK7881	26.5 ± 0.9 (73)	2.01 ± 0.58 (15)	0.85 ± 0.21	4.1 ± 0.7
Δ*frzCD* mutant DW706	22.3 ± 1.0 (55)	2.78 ± 0.68 (30)	0[c]	4.1 ± 0.3
Δ*frzF* mutant DZ4483	17.7 ± 0.8 (83)	Not measured	0.63[d]	Not measured
Δ*frzG* mutant DZ4482	21.1 ± 1.0 (59)	Not measured	1.45[d]	Not measured

[a] Pause durations are average values ± 1 standard error. All other values are averages ± 1 standard deviation. The values in parentheses are numbers of cells tracked.
[b] Calculated from three replicates of each strain.
[c] DW706 exhibits no overall expansion when hyperreversing—all replicates showed no expansion.
[d] Measured in reference 44.

in contact with other cells and dividing cells that were isolated. While predivision cells that stop do not remain absolutely fixed to the surface, these cells do not join in clusters of motile cells upon cell-cell contact, as their neighbors do (see Movie S2). Clearly, these predivision cells are able to dissociate from exopolysaccharide-, cell wall-, and pilus-dependent associations of not just their own but also other cells to facilitate these pauses. In all of the dividing cells we tracked in our experiments, the behavior and regulation of cell division were dominant over numerous motility and cell-cell phenotypes that have been documented under similar growth conditions.

Predivision pauses involve Frz but are independent of S motility. We tracked the motility and divisions of selected motility mutants to probe for factors that are important to the regulation of these predivision pauses. Because these strains are known to display differing motility and growth characteristics, we measured the motility and growth attributes of these strains under the growth conditions used in these experiments (Table 2). Of the

mutants examined, only the Δ*frzE* and Δ*frzCD* mutants show a significant deviation in stoppage from wild-type cells—the predivision pauses of the Δ*frzE* and Δ*frzCD* mutant strains were 26.5 ± 0.9 and 22.3 ± 1.0 min, respectively (Fig. 3). The predivision pauses of the Δ*frzF* and Δ*frzG* mutant strains are statistically similar to those of the wild-type strains. Similar pausing behavior is also detailed for a Δ*pilA* mutant strain that has no TFP; thus, TFP are not needed for this behavior and likely function only after cell division is complete.

Differences in gliding speed, swarm expansion rate, or growth rate did not correlate with the length of the predivisional pause. As we have described above, the pause durations for the division events of DK1622 wild-type, DZ2 wild-type, and DK8621 Δ*pilA* S motility mutant cells are essentially the same (~19 min). Because these strains are known to display differing motility and growth characteristics, we measured both the motility and growth attributes of these strains under the growth conditions used in these experiments (Table 2). No attribute or pattern emerged that correlates with the pause duration for division, and we are unable to explain the notable variation in the pause periods of these predivision cells (Fig. 3). The surface growth rate of DK1622 (and DK1622 mutant) cells is marginally lower than that of DZ2 cells under the growth conditions used here, which is comparable to other studies (48–51). The minimum doubling times of DK1622 and DZ2 are 4.8 ± 0.6 and 3.6 ± 0.1 h, respectively.

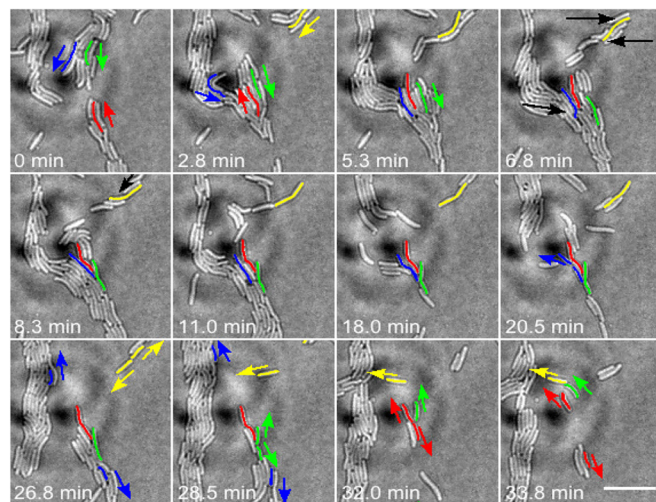**Dividing cells inherit polarity.** We demonstrate that after *M.*

FIG 2 Sequence of motility pausing and cell division in four *M. xanthus* DZ2 cells within a group. Initially (0 to 2.8 min), all of the cells are motile. At 5.3 min, the cells colored blue, red, and yellow have stopped. The green cell stops by 6.8 min, while many other cells remain motile. From 6.8 to 18.0 min, these colored cells do not actively move but are subject to numerous interactions with surrounding active cells (black arrows)—this results in some change in the position of the paused cells. At 20.5 min, the blue cells have divided and initiated motility. The remaining colored cells initiate motility by 32.0 min. Scale bar, 10 μm.
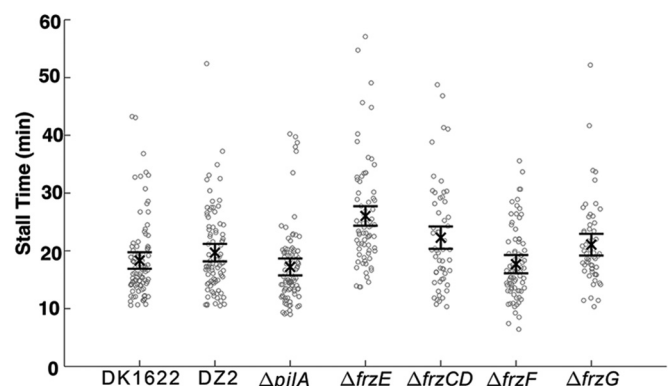

FIG 3 Duration of motility pauses at the time of *M. xanthus* cell division. The mean value of each strain is indicated by the ×, and error bars show the standard error of the 95% confidence interval determined by comparison of the mean values of all of the data points.
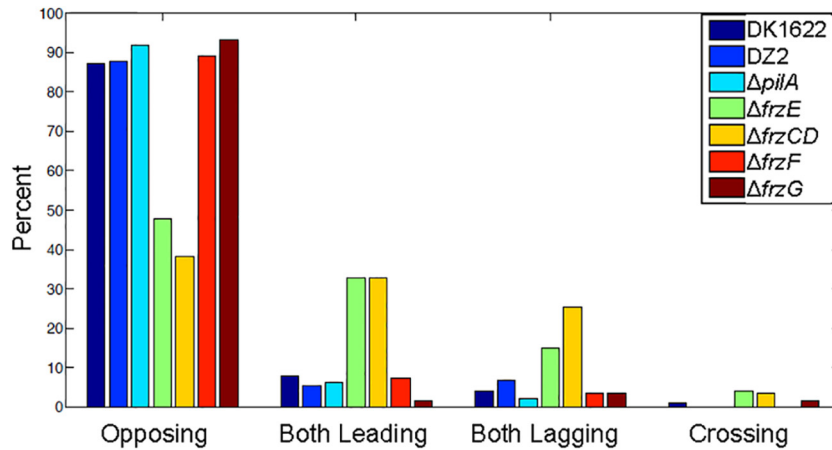
FIG 4 Initial motility directions of both progeny cells with reference to the parent cell as a percentage of the total number of division events of each individual strain. "Opposing," cells initiate motility in opposing directions where the leading cell inherits the motility direction of the parent cell. "Both leading," both cells initiate motility in the direction of the parent cell. "Both lagging," both cells initiate motility in the direction opposite that of the parent cell. "Crossing," cells initiate motility in opposing directions where the lagging cell inherits the motility direction of the parent cell.

xanthus binary cell division is complete and progeny cells separate, they are programmed to move in opposite directions. Newly divided cells were categorized according to their direction of movement. In both the wild-type and Δ*pilA* mutant strains, the leading cell (in reference to the orientation of the predivision cell) moved in the same direction as the parent cell and the lagging cell moved in the opposite direction in approximately 90% of the recorded events (Fig. 4). In nearly all of the remaining events (~10% of the total), the two progeny cells initiated movement in the same direction (see Movie S3 in the supplemental material), with no obvious bias toward the leading or lagging cell direction. In just 1 out of 288 division events tracked in these strains, a "crossing" phenotype was observed where the leading and lagging cells crossed each other. No distinct bias was apparent in the timing of movement after division, as progeny cell pairs resumed movement with either cell starting first or progeny cells initiating movement at the same time (see Fig. S1 in the supplemental material). Two of the four Frz system reversal mutants also showed markedly less asymmetry of motility polarity; these *frzCD* and *frzE* mutant progeny cells were as likely to initiate movement in the direction of the parent (leading) cell as to move in opposite directions (Fig. 4). The

frzG and *frzF* mutant progeny cells exhibit the same initial movement patterns as the wild type.

Distribution of RomR is asymmetric in new poles at division. Our analysis detected no unique behavioral traits (such as a change in velocity) in predivision or newly divided cells in comparison to other *M. xanthus* cells. However, we found that the intracellular localization of motility proteins was cued with the pausing of predivision cells. We investigated the dynamics of the protein RomR during cell division; RomR is known to interact with both the Frz system and the G-protein switch of MglA/MglB that mediate *M. xanthus* reversals (27, 28) and is thought to become localized to poles when nonphosphorylated but to be released from poles when phosphorylated (52). Inspection of RomR-GFP fusions showed that recruitment of RomR to the middle of predivisional cells begins shortly after a mother cell pauses motility for division (Fig. 5; for the entire time-lapse series, see Movie S4 in the supplemental material). This recruitment of RomR to the site of division occurs while the distribution of RomR at the poles of the parent cell (showing higher levels of RomR present at the lagging pole) is nearly static. Most remarkably, the recruitment of RomR at the site of division shows a strik-
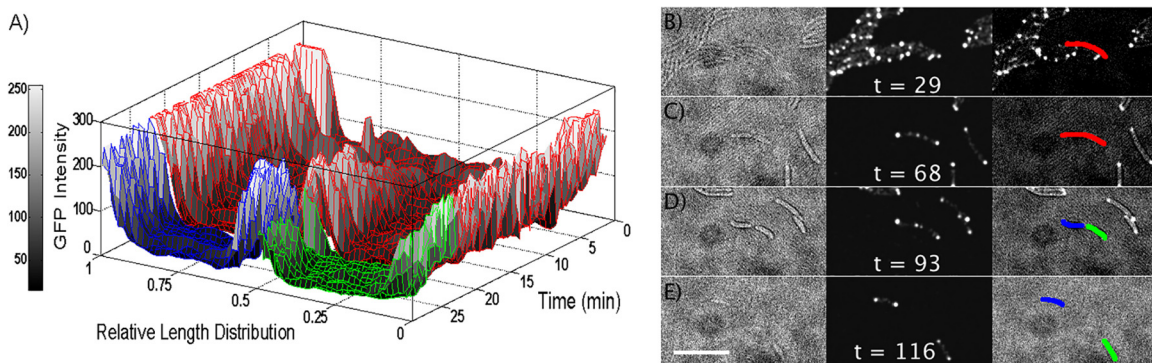

FIG 5 Dynamic distribution of RomR-GFP during the division of a representative cell (colored red) that was initially moving left to right. (A) Fluorescence intensity of RomR-GFP along a dividing cell (longitudinal axis) over time. Cell motility pauses at 2.5 min, and progeny cells initiate motility at 22.5 min. After division, the leading cell (green) moves to the right while the lagging cell (blue) moves to the left. (B to E) Transmission detection image, green fluorescent image, and merged image with delineated cell morphology at 5.75 min (B), 17.0 min (C), 23.25 min (D), and 26.5 min (E).
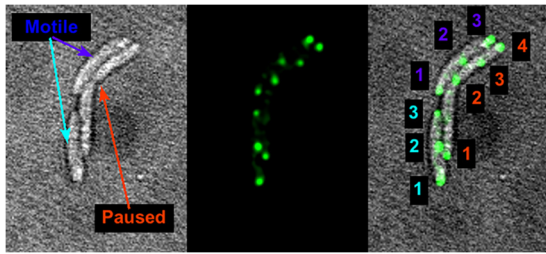
FIG 6 Multipoint accumulation of RomR-GFP in *M. xanthus frzCD* mutant strain JS2. Shown from left to right are the transmission detection image highlighting a paused predivision cell and two other cells, the fluorescence channel showing RomR-GFP, and the merged image with the cell delineation overlay highlighting the three or four RomR accumulation sites of each of these cells.

ing asymmetry between the two progeny cells. The level of asymmetry in RomR distribution at the old poles of the parent cell becomes mirrored in the new poles at the site of division, which we measured by using RomR-GFP (see Fig. S2 in the supplemental material). While the actual RomR leading/lagging pole ratio varies (from 0.43 to 0.83), the mirroring of these levels in new progeny cells is very consistent (ratio of 1.06 ± 0.2 new poles inheriting old-pole RomR in both progeny cells). The RomR-GFP level at the cell midpoint increases from 20 to 40% (relative to the lagging pole) during the pause. As the progeny cells begin to pull apart, the new lagging cell (which initiates movement in the opposite direction) exhibits much higher levels of RomR at the newly formed pole than at the new pole of the leading cell. Thus, RomR is preferentially directed to a specific side at the site of division while the relative abundance of RomR at the previous cell poles is essentially unchanged. Furthermore, the RomR-GFP level at the new pole of the leading cell is approximately 45% of that at the new pole of the lagging cell for the first minute after separation. The RomR-GFP of this lagging-cell new pole then abruptly doubles. Such front-abundant distributions of RomR within motile cells are counterintuitive to our current understanding of the role of RomR in establishing the polarity of motility of *M. xanthus* (27, 53). Previously, it would have been predicted that RomR should be most abundant at the rear pole of motile cells. Here we noted that the newly divided lagging cell initiates opposing motility despite having lower levels of RomR at the newly formed lagging pole than at the leading pole (i.e., the previously lagging pole of the parent cell). Also, the leading cell, which retains the same polarity as the parent cell, is able to resume motility in this direction despite a lack of RomR abundance at the cell rear. Thus, RomR appears to be needed to establish motility in a new direction but not to resume an existing polarity. After 3 to 5 min of motion postdivision, the lagging pole of each of these progeny cells establishes a RomR level greater than or equal to that at the leading pole.

The necessity of proper RomR accumulation at the poles to set opposing polarities in new progeny cells was confirmed by monitoring RomR-GFP in a *frzCD* mutant strain. In a *frzCD* mutant background, *M. xanthus* progeny cells do not necessarily move in opposing directions (Fig. 4) and the Frz system that guides RomR accumulation is disrupted (27, 28). We found that the localization of RomR in a *frzCD* mutant was altered throughout the cell cycle as RomR clusters were observed at multiple locations within all of the cells in a field of view (Fig. 6). In addition to RomR-GFP localized to poles at various ratios, a total of three or four RomR

accumulation sites were observed. Thus, a proper polarity of RomR is never established and progeny cells have a more random polarity after division (see Movie S5 in the supplemental material). Over time, the highest-intensity RomR-GFP does not appreciably oscillate in this *frzCD* mutant strain as in the wild type, suggesting that disassembly of RomR puncta is distorted in this *frzCD* mutant background.

DISCUSSION

Using high-resolution time-lapse microscopy to image the motility of approximately 12,000 *M. xanthus* cells, we found that all dividing cells paused prior to division. We confirmed this behavior for the most commonly studied *M. xanthus* wild-type backgrounds, DK1622 and DZ2. Our analysis detected no unique traits in predivision cells prior to their pausing or in new motile progeny cells in comparison to the other *M. xanthus* cells. We further demonstrated that after division, progeny cells move in opposing directions. These pausing and polarity behaviors involve the Frz cascade, as *frzCD* and *frzE* mutations disrupted these patterns. We conclude that this behavior involves *M. xanthus* A motility, as a *pilA*-deficient S motility mutant exhibited the same behavior as the wild type.

The requirement and duration of these pauses were notably unaffected by physical interactions with other *M. xanthus* cells. This suggests a layer of complexity in the associations of *M. xanthus* and other organisms that has not been considered previously—promotion of intercellular activity by neighboring cells can be both blocked and undone by predivision cells. Several studies have shown the importance of different biochemical and physical components that promote cell-cell interaction (11, 18, 21, 22, 44, 54–56), group alignment (21, 44, 56), and group motility (19, 20, 44, 57, 58) of *M. xanthus*. However, our results show that pausing for cell division dominates over any tested intercellular interactions, with no distinction between the pausing behavior of dividing cells that were in contact with other cells and that of dividing cells that were isolated. Clearly, predivision cells are able to dissociate from the polysaccharide-, cell wall-, and pilus-dependent associations of not just their own but also other cells to facilitate these pauses. This suggests a layer of complexity in such associations that has not been considered previously—we found that the behavior and regulation of cell division are dominant over numerous motility and cell-cell phenotypes such that promotion of intercellular activity by neighboring cells can be both blocked and undone by predivision cells. While these predivision pauses were independent of S motility, any pilus-mediated effects actually appear to be negated as *M. xanthus* pauses for division.

While most *M. xanthus* progeny cells displayed these asymmetric polarity traits, the timing of their movement showed no clear pattern. After division, the predominant phenotype observed was for both cells to initiate movement at essentially the same time. The novelty of this synchronous or unfavored timing is not yet clear, as few studies have examined the onset of motility in newly divided cells. Certainly, *Caulobacter crescentus* shows highly asynchronous behavior, as one attached cell yields one motile cell during division (1). Somewhat similarly, it has been shown that one divided cell of the TFP-motile bacterium *P. aeruginosa* remains attached in surface-attached division events while the other may be motile (59).

The specific mechanism and dynamics of *M. xanthus* cell division, like those of most nonmodel organisms, are not entirely
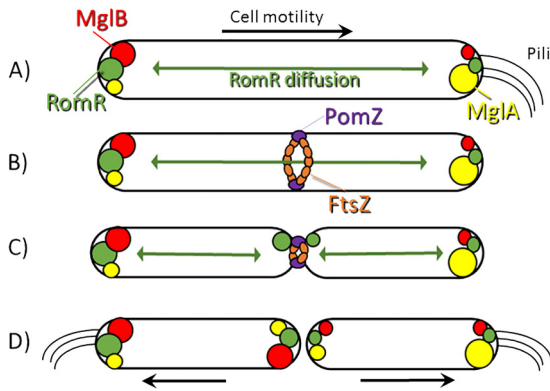
FIG 7 Model of cell division and polarity inheritance via diffusion of RomR in *M. xanthus*. (A) A motile predivision cell moves left to right. RomR is localized to both poles but preferentially to the rear pole, while phosphorylated RomR (RomR~P) is freely diffused in the cytoplasm. (B) The predivisional cell pauses its motility. Key division proteins PomZ and FtsZ act to mark the cell division site and initiate separation. (C) As FtsZ constricts the cell, this both limits the diffusion of RomR~P across the entire volume and cues the accumulation of RomR at these newly developing poles. RomR preferentially accumulates at the new pole of the lagging cell. (D) Upon completion of cell division, these progeny cells display sufficiently differing polar traits to initiate motility in opposing directions. Synthesis of new TFP may coincide with these actions, but they are not required to initiate motility.

known. *M. xanthus* is among many bacteria lacking a clear MinCD system that drives the recruitment of FtsZ for division. It is known that the middle of *M. xanthus* cells is marked by the ParA-like protein PomZ (7). There is support for an association of PomZ with setting of *M. xanthus* motility, as *pomZ* (originally annotated as *agmE*) was originally identified as a partial A motility mutation.

We describe the resetting of *M. xanthus* polarity at division by correlating the accumulation of RomR at newly formed cell poles with cell division (Fig. 7). Our results are consistent with an explanation that pausing of motility is a well-ordered step of the cell cycle. Recent evidence of the detailed orchestration of ParA/ParB important to chromosomal segregation suggests a distinct cycle of approximately 4 h where division into two cells accounts for 30 to 60 min (60, 61). On the basis of our results, we link cell division with the establishment of opposing motility polarity in progeny cells by considering the possible RomR distribution scenarios. We assume that sufficient phosphorylated RomR is diffused freely throughout the cell (Fig. 7). As the motility of these predivision cells is paused, we deduce from our experiments that RomR has not yet begun to accumulate via dephosphorylation at the site of division (Fig. 5) but continues to diffuse freely in the phosphorylated state. However, we propose that diffusion across the entire predivisional cell starts to become limited at this stage (Fig. 7C) because of the constriction of cell division, limiting flow between the two cell ends. This constriction also introduces a morphology change as curvature at the predivisional cell middle is initiated—we propose that RomR recognizes some component of this developing cell pole, as it must recognize existing poles. This may be directly associated with *M. xanthus* ParA, which is known to localize to cell poles and sites of division (60, 61). While diffusion of RomR continues, the level of asymmetry in RomR distribution at the old poles of the parent cell is mirrored in the new poles at the site of division, which we measured by using RomR-GFP (see Fig. S2 in the supplemental material). While the actual ratio of mea-

sured leading/lagging pole RomR levels of any single cell varies (from 0.43 to 0.83), the mirroring of these levels from parent to progeny cells is very consistent (ratio of 1.06 ± 0.2 new poles inheriting old-pole RomR in both progeny cells). Upon the completion of cell division, the accumulation of RomR in the lagging cell is sufficient to recruit MglB to initiate a new direction, explaining why we saw progeny cells move away from each other following division.

Morphologically symmetrical *M. xanthus* cells inherit a clear asymmetry in the distribution of proteins that confer their motility. We propose that this asymmetry is mirrored at the parent cell midpoint because of the process of division to explain the opposing polarity we observed when division was complete. This proposed mechanism would be sensitive at the time of motility pausing to the distribution of RomR, which is known to switch from the asymmetric pattern to a short-lived symmetric pattern to the opposite asymmetric pattern during cell directional reversals (52). Thus, disruption of the Frz system, which affects reversal timing, would be expected to disrupt the polarity pattern inherited by daughter cells, as seen in our experiments. Because most cell types are symmetrical, like the *M. xanthus* cells we examined here, gaining more insight into the coordination cascade that regulates this phenotype may useful in understanding other processes that are associated with cell division.

ACKNOWLEDGMENTS

REFERENCES

1. **Hughes V, Jiang C, Brun Y.** 2012. *Caulobacter crescentus.* Curr. Biol. **22:**R507–R509. http://dx.doi.org/10.1016/j.cub.2012.05.036.
2. **Kirsebom LA, Dasgupta S, Fredrik Pettersson BM.** 2012. Pleiomorphism in *Mycobacterium.* Adv. Appl. Microbiol. **80:**81–112. http://dx.doi.org/10.1016/B978-0-12-394381-1.00004-0.
3. **Horvitz HR, Herskowitz I.** 1992. Mechanisms of asymmetric cell division: two Bs or not two Bs, that is the question. Cell **68:**237–255. http://dx.doi.org/10.1016/0092-8674(92)90468-R.
4. **Brown PJB, Kysela DT, Brun YV.** 2011. Polarity and the diversity of growth mechanisms in bacteria. Semin. Cell Dev. Biol. **22:**790–798. http://dx.doi.org/10.1016/j.semcdb.2011.06.006.
5. **Reichenbach H.** 1999. The ecology of the myxobacteria. Environ. Microbiol. **1:**15–21. http://dx.doi.org/10.1046/j.1462-2920.1999.00016.x.
6. **Berleman JE, Scott J, Chumley T, Kirby JR.** 2008. Predataxis behavior in *Myxococcus xanthus.* Proc. Natl. Acad. Sci. U. S. A. **105:**17127–17132. http://dx.doi.org/10.1073/pnas.0804387105.
7. **Treuner-Lange A, Aguiluz K, van der Does C, Gómez-Santos N, Harms A, Schumacher D, Lenz P, Hoppert M, Kahnt J, Muñoz-Dorado J, Søgaard-Andersen L.** 2013. PomZ, a ParA-like protein, regulates Z-ring formation and cell division in *Myxococcus xanthus.* Mol. Microbiol. **87:**235–253. http://dx.doi.org/10.1111/mmi.12094.
8. **Campos JM, Zusman DR.** 1975. Regulation of development in *Myxococcus xanthus*: effect of 3′:5′-cyclic AMP, ADP, and nutrition. Proc. Natl. Acad. Sci. U. S. A. **72:**518–522. http://dx.doi.org/10.1073/pnas.72.2.518.
9. **Xie C, Zhang H, Shimkets LJ, Igoshin OA.** 2011. Statistical image analysis reveals features affecting fates of *Myxococcus xanthus* developmental aggregates. Proc. Natl. Acad. Sci. U. S. A. **108:**5915–5920. http://dx.doi.org/10.1073/pnas.1018383108.
10. **Zhang H, Angus S, Tran M, Xie C, Igoshin OA, Welch RD.** 2011. Quan-

tifying aggregation dynamics during *Myxococcus xanthus* development. J. Bacteriol. **193:**5164–5170. http://dx.doi.org/10.1128/JB.05188-11.

11. **Dana JR, Shimkets LJ.** 1993. Regulation of cohesion-dependent cell interactions in *Myxococcus xanthus*. J. Bacteriol. **175:**3636–3647.

12. **Sozinova O, Jiang Y, Kaiser D, Alber M.** 2006. A three-dimensional model of myxobacterial fruiting-body formation. Proc. Natl. Acad. Sci. U. S. A. **103:**17255–17259. http://dx.doi.org/10.1073/pnas.0605555103.

13. **Harvey CW, Du H, Xu Z, Kaiser D, Aranson I, Alber M.** 2012. Interconnected cavernous structure of bacterial fruiting bodies. PLoS Comput. Biol. **8**(12):e1002850. http://dx.doi.org/10.1371/journal.pcbi .1002850.

14. **Koch MK, Hoiczyk E.** 2013. Characterization of myxobacterial A-motility: insights from microcinematographic observations. J. Basic Microbiol. **53:**785–791. http://dx.doi.org/10.1002/jobm.201200307.

15. **Kaiser D, Robinson M, Kroos L.** 2010. Myxobacteria, polarity, and multicellular morphogenesis. Cold Spring Harb. Perspect. Biol. **2**(8): a000380. http://dx.doi.org/10.1101/cshperspect.a000380.

16. **Balagam R, Litwin DB, Czerwinski F, Sun M, Kaplan HB, Shaevitz JW, Igoshin OA.** 2014. *Myxococcus xanthus* gliding motors are elastically coupled to the substrate as predicted by the focal adhesion model of gliding motility. PLoS Comput. Biol. **10**(5):e1003619. http://dx.doi.org/10.1371 /journal.pcbi.1003619.

17. **Nan B, Zusman DR.** 2011. Uncovering the mystery of gliding motility in the myxobacteria. Annu. Rev. Genet. **45:**21–39. http://dx.doi.org/10.1146 /annurev-genet-110410-132547.

18. **Kaiser D.** 1979. Social gliding is correlated with the presence of pili in *Myxococcus xanthus*. Proc. Natl. Acad. Sci. U. S. A. **76:**5952–5956. http: //dx.doi.org/10.1073/pnas.76.11.5952.

19. **Youderian P, Hartzell PL.** 2007. Triple mutants uncover three new genes required for social motility in *Myxococcus xanthus*. Genetics **177:**557–566. http://dx.doi.org/10.1534/genetics.107.076182.

20. **Lu A, Cho K, Black WP, Duan X-y, Lux R, Yang Z, Kaplan HB, Zusman DR, Shi W.** 2005. Exopolysaccharide biosynthesis genes required for social motility in *Myxococcus xanthus*. Mol. Microbiol. **55:**206–220. http: //dx.doi.org/10.1111/j.1365-2958.2004.04369.x.

21. **Wu YL, Kaiser AD, Jiang Y, Alber MS.** 2009. Periodic reversal of direction allows myxobacteria to swarm. Proc. Natl. Acad. Sci. U. S. A. **106:** 1222–1227. http://dx.doi.org/10.1073/pnas.0811662106.

22. **Mauriello EM, Astling DP, Sliusarenko O, Zusman DR.** 2009. Localization of a bacterial cytoplasmic receptor is dynamic and changes with cell-cell contacts. Proc. Natl. Acad. Sci. U. S. A. **106:**4852–4857. http://dx.doi .org/10.1073/pnas.0810583106.

23. **Yu R, Kaiser D.** 2007. Gliding motility and polarized slime secretion. Mol. Microbiol. **63:**454–467. http://dx.doi.org/10.1111/j.1365-2958 .2006.05536.x.

24. **Leonardy S, Miertzschke M, Bulyha I, Sperling E, Wittinghofer A, Søgaard-Andersen L.** 2010. Regulation of dynamic polarity switching in bacteria by a Ras-like G-protein and its cognate GAP. EMBO J. **29:**2276– 2289. http://dx.doi.org/10.1038/emboj.2010.114.

25. **Zhang Y, Franco M, Ducret A, Mignot T.** 2010. A bacterial Ras-like small GTP-binding protein and its cognate GAP establish a dynamic spatial polarity axis to control directed motility. PLoS Biol. **8**(7):e1000430. http: //dx.doi.org/10.1371/journal.pbio.1000430.

26. **Blackhart BD, Zusman DR.** 1985. "Frizzy" genes of *Myxococcus xanthus* are involved in control of frequency of reversal of gliding motility. Proc. Natl. Acad. Sci. U. S. A. **82:**8767–8770. http://dx.doi.org/10.1073/pnas.82 .24.8767.

27. **Keilberg D, Wuichet K, Drescher F, Søgaard-Andersen L.** 2012. A response regulator interfaces between the Frz chemosensory system and the MglA/MglB GTPase/GAP module to regulate polarity in *Myxococcus xanthus*. PLoS Genet. **8**(9):e1002951. http://dx.doi.org/10.1371/journal .pgen.1002951.

28. **Zhang Y, Guzzo M, Ducret A, Li Y-Z, Mignot T.** 2012. A dynamic response regulator protein modulates G-protein-dependent polarity in the bacterium *Myxococcus xanthus*. PLoS Genet. **8**(8):e1002872. http://dx .doi.org/10.1371/journal.pgen.1002872.

29. **Bustamante VH, Martinez-Flores I, Vlamakis HC, Zusman DR.** 2004. Analysis of the Frz signal transduction system of *Myxococcus xanthus* shows the importance of the conserved C-terminal region of the cytoplasmic chemoreceptor FrzCD in sensing signals. Mol. Microbiol. **53:**1501– 1513. http://dx.doi.org/10.1111/j.1365-2958.2004.04221.x.

30. **Inclán YF, Laurent S, Zusman DR.** 2008. The receiver domain of FrzE, a CheA-CheY fusion protein, regulates the CheA histidine kinase activity

31. **Scott AE, Simon E, Park SK, Andrews P, Zusman DR.** 2008. Site-specific receptor methylation of FrzCD in *Myxococcus xanthus* is controlled by a tetra-trico peptide repeat (TPR) containing regulatory domain of the FrzF methyltransferase. Mol. Microbiol. **69:**724–735. http://dx.doi.org/10 .1111/j.1365-2958.2008.06323.x.

32. **Wadhams GH, Armitage JP.** 2004. Making sense of it all: bacterial chemotaxis. Nat. Rev. Mol. Cell Biol. **5:**1024–1037. http://dx.doi.org/10.1038 /nrm1524.

33. **Wolfe AJ, Conley MP, Kramer TJ, Berg HC.** 1987. Reconstitution of signaling in bacterial chemotaxis. J. Bacteriol. **169:**1878–1885.

34. **Hickman JW, Tifrea DF, Harwood CS.** 2005. A chemosensory system that regulates biofilm formation through modulation of cyclic diguanylate levels. Proc. Natl. Acad. Sci. U. S. A. **102:**14422–14427. http://dx.doi.org /10.1073/pnas.0507170102.

35. **Huangyutitham V, Guvener ZT, Harwood CS.** 2013. Subcellular clustering of the phosphorylated WspR response regulator protein stimulates its diguanylate cyclase activity. mBio **4**(3):e00242–00213. http://dx.doi .org/10.1128/mBio.00242-13.

36. **O'Connor JR, Kuwada NJ, Huangyutitham V, Wiggins PA, Harwood CS.** 2012. Surface sensing and lateral subcellular localization of WspA, the receptor in a chemosensory-like system leading to c-di-GMP production. Mol. Microbiol. **86:**720–729. http://dx.doi.org/10.1111/mmi.12013.

37. **Bulyha I, Lindow S, Lin L, Bolte K, Wuichet K, Kahnt J, van der Does C, Thanbichler M, Søgaard-Andersen L.** 2013. Two small GTPases act in concert with the bactofilin cytoskeleton to regulate dynamic bacterial cell polarity. Dev. Cell **25:**119–131. http://dx.doi.org/10.1016/j.devcel.2013 .02.017.

38. **Kaimer C, Zusman DR.** 2013. Phosphorylation-dependent localization of the response regulator FrzZ signals cell reversals in *Myxococcus xanthus*. Mol. Microbiol. **88:**740–753. http://dx.doi.org/10.1111/mmi.12219.

39. **Nudleman E, Wall D, Kaiser D.** 2006. Polar assembly of the type IV pilus secretin in Myxococcus xanthus. Mol. Microbiol. **60:**16–29. http://dx.doi .org/10.1111/j.1365-2958.2006.05095.x.

40. **Bulyha I, Schmidt C, Lenz P, Jakovljevic V, Hone A, Maier B, Hoppert M, Søgaard-Andersen L.** 2009. Regulation of the type IV pili molecular machine by dynamic localization of two motor proteins. Mol. Microbiol. **74:**691–706. http://dx.doi.org/10.1111/j.1365-2958.2009.06891.x.

41. **Hodgkin J, Kaiser D.** 1977. Cell-to-cell stimulation of movement in nonmotile mutants of *Myxococcus*. Proc. Natl. Acad. Sci. U. S. A. **74:**2938– 2942. http://dx.doi.org/10.1073/pnas.74.7.2938.

42. **Taylor RG, Welch RD.** 2010. Recording multicellular behavior in *Myxococcus xanthus* biofilms using time-lapse microcinematography. J. Vis. Exp. **42:**2038. http://dx.doi.org/10.3791/2038.

43. **Morris JD, Hewitt JL, Wolfe LG, Kamatkar NG, Chapman SM, Diener JM, Courtney AJ, Leevy WM, Shrout JD.** 2011. Imaging and analysis of *Pseudomonas aeruginosa* swarming and rhamnolipid production. Appl. Environ. Microbiol. **77:**8310–8317. http://dx.doi.org/10.1128 /AEM.06644-11.

44. **Kaiser D, Warrick H.** 2011. *Myxococcus xanthus* swarms are driven by growth and regulated by a pacemaker. J. Bacteriol. **193:**5898–5904. http: //dx.doi.org/10.1128/JB.00168-11.

45. **Reichenbach H, Heunert HH, Kuczka H.** 1965. Myxococcus spp. (Myxobacterales)-Schwarmentwicklung und Bildung von Protocysten. Institut fur den Wissenschaftlichen Film, Göttingen, Federal Republic of Germany.

46. **Mignot T, Shaevitz JW, Hartzell PL, Zusman DR.** 2007. Evidence that focal adhesion complexes power bacterial gliding motility. Science **315:** 853–856. http://dx.doi.org/10.1126/science.1137223.

47. **Mignot T, Merlie JP, Jr, Zusman DR.** 2005. Regulated pole-to-pole oscillations of a bacterial gliding motility protein. Science **310:**855–857. http://dx.doi.org/10.1126/science.1119052.

48. **Kimchi A, Rosenberg E.** 1976. Linkages between deoxyribonucleic acid synthesis and cell division in *Myxococcus xanthus*. J. Bacteriol. **128:**69–79.

49. **Rosario CJ, Singer M.** 2007. The *Myxococcus xanthus* developmental program can be delayed by inhibition of DNA replication. J. Bacteriol. **189:**8793–8800. http://dx.doi.org/10.1128/JB.01361-07.

50. **Sun H, Yang Z, Shi W.** 1999. Effect of cellular filamentation on adventurous and social gliding motility of *Myxococcus xanthus*. Proc. Natl. Acad. Sci. U. S. A. **96:**15178–15183. http://dx.doi.org/10.1073/pnas .96.26.15178.

51. **Tzeng L, Ellis TN, Singer M.** 2006. DNA replication during aggregation phase is essential for *Myxococcus xanthus* development. J. Bacteriol. **188:** 2774–2779. http://dx.doi.org/10.1128/JB.188.8.2774-2779.2006.

52. **Leonardy S, Freymark G, Hebener S, Ellehauge E, Søgaard-Andersen L.** 2007. Coupling of protein localization and cell movements by a dynamically localized response regulator in *Myxococcus xanthus*. EMBO J. **26:** 4433–4444. http://dx.doi.org/10.1038/sj.emboj.7601877.

53. **Zhang Y, Guzzo M, Ducret A, Li YZ, Mignot T.** 2012. A dynamic response regulator protein modulates G-protein-dependent polarity in the bacterium *Myxococcus xanthus*. PLoS Genet. **8**(8):e1002872. http://dx.doi.org/10.1371/journal.pgen.1002872.

54. **Bowden MG, Kaplan HB.** 1998. The *Myxococcus xanthus* lipopolysaccharide O-antigen is required for social motility and multicellular development. Mol. Microbiol. **30:**275–284. http://dx.doi.org/10.1046/j.1365-2958.1998.01060.x.

55. **Pathak DT, Wei X, Bucuvalas A, Haft DH, Gerloff DL, Wall D.** 2012. Cell contact-dependent outer membrane exchange in myxobacteria: genetic determinants and mechanism. PLoS Genet. **8**(4):e1002626. http://dx.doi.org/10.1371/journal.pgen.1002626.

56. **Pathak DT, Wall D.** 2012. Identification of the *cglC*, *cglD*, *cglE*, and *cglF* genes and their role in cell contact-dependent gliding motility in *Myxococcus xanthus*. J. Bacteriol. **194:**1940–1949. http://dx.doi.org/10.1128/JB.00055-12.

57. **Dworkin M, Kaiser D.** 1985. Cell interactions in myxobacterial growth and development. Science **230:**18–24. http://dx.doi.org/10.1126/science.3929384.

58. **Wu Y, Jiang Y, Kaiser D, Alber M.** 2007. Social interactions in myxobacterial swarming. PLoS Comput. Biol. **3**(12):e253. http://dx.doi.org/10.1371/journal.pcbi.0030253.

59. **Conrad JC, Gibiansky ML, Jin F, Gordon VD, Motto DA, Mathewson MA, Stopka WG, Zelasko DC, Shrout JD, Wong GC.** 2011. Flagella and pili-mediated near-surface single-cell motility mechanisms in *P. aeruginosa*. Biophys. J. **100:**1608–1616. http://dx.doi.org/10.1016/j.bpj.2011.02.020.

60. **Harms A, Treuner-Lange A, Schumacher D, Søgaard-Andersen L.** 2013. Tracking of chromosome and replisome dynamics in *Myxococcus xanthus* reveals a novel chromosome arrangement. PLoS Genet. **9**(9):e1003802. http://dx.doi.org/10.1371/journal.pgen.1003802.

61. **Iniesta AA.** 2014. ParABS system in chromosome partitioning in the bacterium *Myxococcus xanthus*. PLoS One **9**(1):e86897. http://dx.doi.org/10.1371/journal.pone.0086897.

62. **Wall D, Kolenbrander PE, Kaiser D.** 1999. The *Myxococcus xanthus pilQ* (*sglA*) gene encodes a secretin homolog required for type IV pilus biogenesis, social motility, and development. J. Bacteriol. **181:**24–33.

63. **Kimsey HH, Kaiser D.** 1991. Targeted disruption of the *Myxococcus xanthus* orotidine 5′-monophosphate decarboxylase gene: effects on growth and fruiting-body development. J. Bacteriol. **173:**6790–6797.